High Performance Ternary Organic Solar Cells Due to Favored Interfacial Connection by a Non-Fullerene Electron Acceptor with Cross-Like Molecular Geometry

Journal:	*The Journal of Physical Chemistry*
Manuscript ID	jp-2018-03013p
Manuscript Type:	Article
Date Submitted by the Author:	30-Mar-2018

Complete List of Authors:	Sharapov, Valerii; The University of Chicago, Chemistry Wu, Qinghe; Shantou University, chemistry Neshchadin, Andriy; Department of Chemistry and The James Franck Institute, The University of Chicago Zhao, Donglin; The University of Chicago, Department of Chemistry and The James Franck Institute Cai, Zhengxu; Beijing Institute of Technology, School of Materials Science & Engineering Chen, Wei; Argonne National Laboratory, Materials Science Division/Institute for Molecular Engineering Yu, Luping; University of Chicago, Chemistry

High Performance Ternary Organic Solar Cells Due to Favored Interfacial Connection by A Non-Fullerene Electron Acceptor with Cross-like Molecular Geometry

Valerii Sharapov,[†Δ] *Qinghe Wu,* [†◇Δ] *Andriy Neshchadin,* [†] *Donglin Zhao,* [†#] *Zhengxu Cai,* [†] *Wei Chen,* [‡§] *and Luping Yu*[*†].

[†]Department of Chemistry and The James Franck Institute, The University of Chicago, 929 E 57th Street, Chicago, IL 60637, USA

[◇]Department of Chemistry and Key Laboratory for Preparation and Application of Ordered Structural Materials of Guangdong Province, Shantou University, Guangdong 515063, P. R. China.

[‡]Materials Science Division, Argonne National Laboratory, 9700 Cass Avenue, Lemont, Illinois 60439, USA

[§]Institute for Molecular Engineering, the University of Chicago, 5747 South Ellis Avenue, Chicago, Illinois 60637, USA.

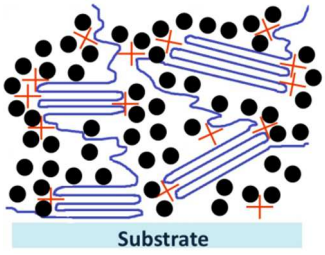

For Table of Contents use only.

ABSTRACT: The non-fullerene electron acceptor, TPB, exhibits the unique cross-like molecular geometry, which helps it to stay preferentially at the interfaces between PTB7-Th and $PC_{71}BM$, when it was used as the third component in ternary OPV cells. The four PDI units connected to TPB's core provide multiple contact points between PTB7-Th and PC71BM phases, thus facilitating interfacial charge extraction and improving overall PCE to 10.6 % from 9.8 % after 10% TPB was added as the third component. This paper describes detailed experimental results and a model to explain these observations.

INTRODUCTION

Bulk heterojunction organic solar cells are very complex system. Numerous parameters, such as molecular structure, blend composition, morphology and device architecture have to be tuned to achieve high power conversion efficiency. A substantial research effort worldwide is devoted to the development of new photovoltaic materials and improvement of device fabrication for better morphology control, higher crystallinity and more efficient light harvesting. As a consequence of these efforts, power conversion efficiencies of organic solar cells have already surpassed a mark of 13% in single heterojunction devices.[1–7] One of the effective approaches to fabricate high efficiency organic photovoltaic devices (OPV) is to utilize multiple donors or multiple acceptors approach in bulk heterojunction (BHJ) solar cells (so called ternary blends). The obvious advantage of this approach is the ability to broaden coverage of the solar spectrum to harvest wider range of photons and minimize the voltage-current trade-off present when only one light absorbing material is used.[8] Another advantage is a possibility of replacing or complementing fullerene derivatives with a better absorbing non-fullerene acceptor (NFA) thus ensuring more efficient photon harvesting in green and blue parts of the spectrum.[8–10] While ternary

blend devices with donor third components (both polymer and small molecule) have been intensively studied before[8,9,11–13], ternary systems with small molecule acceptors are still an emerging field. Early trials in this field involved incorporation of multiple fullerene-based acceptors, such as PCBM and ICBA into a blend. This approach was proven to be effective resulting in an increased performance both for highly crystalline P3HT and more amorphous PTB7.[14,15] More recently, PCBM/ICBA mixture was incorporated into double donor system PTB7:PBDTTA, thus forming a quaternary blend which resulted in a performance increase up to 10.2% PCE, mostly due to complementary light absorption of components, bilateral cascade of energy levels and higher crystallinity of complementary donor polymer.[16] Even though very promising results were achieved with this strategy, possibilities for chemical modification in fullerene-based molecules are very limited, which becomes a bottleneck for further optimization. The non-fullerene acceptors and their use in ternary devices become attractive. In general, to act as an effective third component, a material must exhibit a set of essential properties, including complementary light absorption with a donor, cascade of energy levels for efficient charge transfer and morphological compatibility. More detailed mechanistic studies showed that origin of device efficiency enhancement varies depending on the nature of materials used and the composition of a system. For example, in case of indacenodithiophene based IDTBR and indenofluorene based IDFBR acceptors three distinct phases were observed in the best performing system P3HT:IDFBT:IDTBR (1:0.3:0.7) which also resulted in an increased PCE up to 7.7% PCE. The same acceptor system studied with more amorphous PTB7-Th resulted in >11% PCE.[5] Small molecule acceptors also play an important role in controlling charge carrier mobilities, where more balanced transport of holes and electrons results in devices with better performance.[5,16–21] Another mechanism of enhancement in ternary solar cells is Förster resonance energy transfer (FRET) between components of the blend, therefore matching bandgaps of blend components are crucial for these systems. A typical example is based on squaraine based acceptors (SQ) in

ternary cells as an energy transfer relay. [18,22] Similar strategy applied for planar heterojunction devices with one donor and two subphtalocyanine based acceptors resulted in an enhanced performance due to favorable energy level cascade and FRET between device components.[23] Recently indacenodithiothiopene based (ITIC) family of acceptors were reported as an effective main or third component and higher OPV performance were achieved for systems with higher ratio of ITIC in a blend (> 50% by mass).[19,24,25]

Despite of all the progress made in developing ternary OPV cells, there are still challenges that need to be addressed, especially associated with working mechanism of a third component. The binary OPV cells are already complex systems, and the addition of the third component makes the complexity multiplied. Previously, we reported an electron acceptor (TPB) that has lowest unoccupied molecular orbital (LUMO) energy level very close to that of the $PC_{71}BM$.[26,27] Its highest occupied molecular orbital (HOMO) is higher than that of $PC_{71}BM$ and lower than that of a donor polymer PTB7-Th, forming a hole transport cascade. The suitable molecular energy levels and complementary absorption spectra make TPB an ideal third component candidate for ternary solar cells. It was found that the inverted PTB7-Th/$PC_{71}BM$ OPV devices with TPB as the third component exhibited a PCE as high as 10.6% while PCE for binary devices is 9.8%. The PCE enhancement mainly comes from an increase of J_{sc} values from 17.24 to 19.44 mA/cm^{-2}. The detailed study shows that TPB can act as the interface modifier due to its unique cross-like molecular geometry, which benefits more efficient exciton dissociation and charge separation at donor and acceptor interfaces.

EXPERIMENTAL SECTION

Materials used: Polymer PTB7-Th was purchased from company 1-Material Inc., fullerene based acceptor $PC_{71}BM$ was purchased from American Dye Source Inc. Small molecule acceptor TPB was synthesized in our lab following procedures reported elsewhere.[26] Chlorobenzene, 1.8-diiodooctane, $Zn(CH_3COO)_2{\cdot}2H_2O$, 2-methoxyethanol and 2-aminoethanol all purchased from Sigma-Aldrich. All chemicals were used as obtained from the manufacturer.

Device fabrication: Devices were fabricated in inverted configuration ITO/ZnO/active layer/MoO_3/Ag. ITO substrates, purchased from Thin Film Devices Inc. were ultrasonicated in chloroform, acetone and isopropanol for 15 min and then treated with UV-ozone for 30 min. Sol gel precursor solution of ZnO containing $Zn(CH_3COO)_2{\cdot}2H_2O$ in 2-methoxyethanol and 2-aminoethanol was prepared following procedures described elsewhere.[28] To form a film of ZnO the solution was added dropwise onto ITO substrates through PTFE syringe filter and spin coated at 4000 rpm for 40 seconds. Films were annealed in air immediately after spin coating at 200^0C for 30 minutes. Polymer and small molecule acceptors were dissolved in a chlorobenzene:DIO (97:3 vol %) overnight and solution was spin coated onto the substrates at 70^0 C in a glovebox. Films were immediately transferred to a vacuum chamber and MoO_3 (8 nm) and Ag (80 nm) were thermally evaporated under the pressure lower than 2×10^{-6} Torr.

Device characterization: JV curves of the devices were measured with a source meter unit model Keithley 2420. Devices were tested in nitrogen glovebox under 1 sun conditions (AM1.5G, 100 mW cm^{-2}) using xenon lamp (Oriel 69920) intensity of which was calibrated with a standard NREL certified Si cell (Newport, 91150V). Masks with a well-defined area of 3.14 mm^2 were used to define an active area of the device. Devices for EQE were sealed using UV curable Norland optical adhesive and measured

outside of glovebox. EQE was measured with a Newport QE measurement system (IQE-200) with a tungsten halogen lamp as a light source. To measure light intensity dependent properties a series of neutral density filters was used. To measure charge carrier mobility hole-only devices were fabricated with a structure ITO/PEDOT/active layer/MoO_x/Ag and electron-only device ITO/ZnO/active layer/Ca/Al. JV curves were measured in dark from 0 to 10V and SCLC region was fitted with a Mott-Gurney law equation $J=(9\varepsilon\varepsilon_0\mu(V_{app}-V_{bi})^2/(8L^3)$ where J – current density, ε – dielectric constant of the medium (assumed value 3), μ-mobility, L-thickness. UV/Vis spectra were obtained with Shimadzu UV-2401PC spectrophotometer. PL spectra were obtained with Horiba FluoroLog-3 fluorometer.

Morphology studies: TEM measurements were performed with Tecnai F30 microscope. AFM studies were made with Asylum Cyfer microscope at the University of Chicago MRSEC MPML facilities. AFM was measured in a tapping mode using Arrow UHF tip. The GIWAXS measurements were performed at 8ID-E beamline of Advanced Photon Source, Argonne National Laboratory with a radiation wavelength 1.1364 Å. Samples for GIWAXS were prepared on polished Si wafer, covered with ZnO and coated with an active layer film being studied. Scherer analysis of GIWAXS data was conducted where linecut peaks were fitted with pseudo-Voigt function to determine peak's position and full width at half maximum (FWHM).

Surface energy measurements: Contact angle measurements were performed on pristine films of PTB7-Th, $PC_{71}BM$ and TPB using drop shape analyzer DSA-100 from Krüss GmbH at the University of Chicago MRSEC MPML. Experiments were conducted in air at room temperature for ultrapure 18MΩ water, diiodomethane and ethylene glycol. Software provided with the machine was used to analyze data and calculate surface energies for these materials using the OWRK (Owens, Wendt, Rabel and Kaelble) model.

RESULTS AND DISCUSSION.

OPV performance

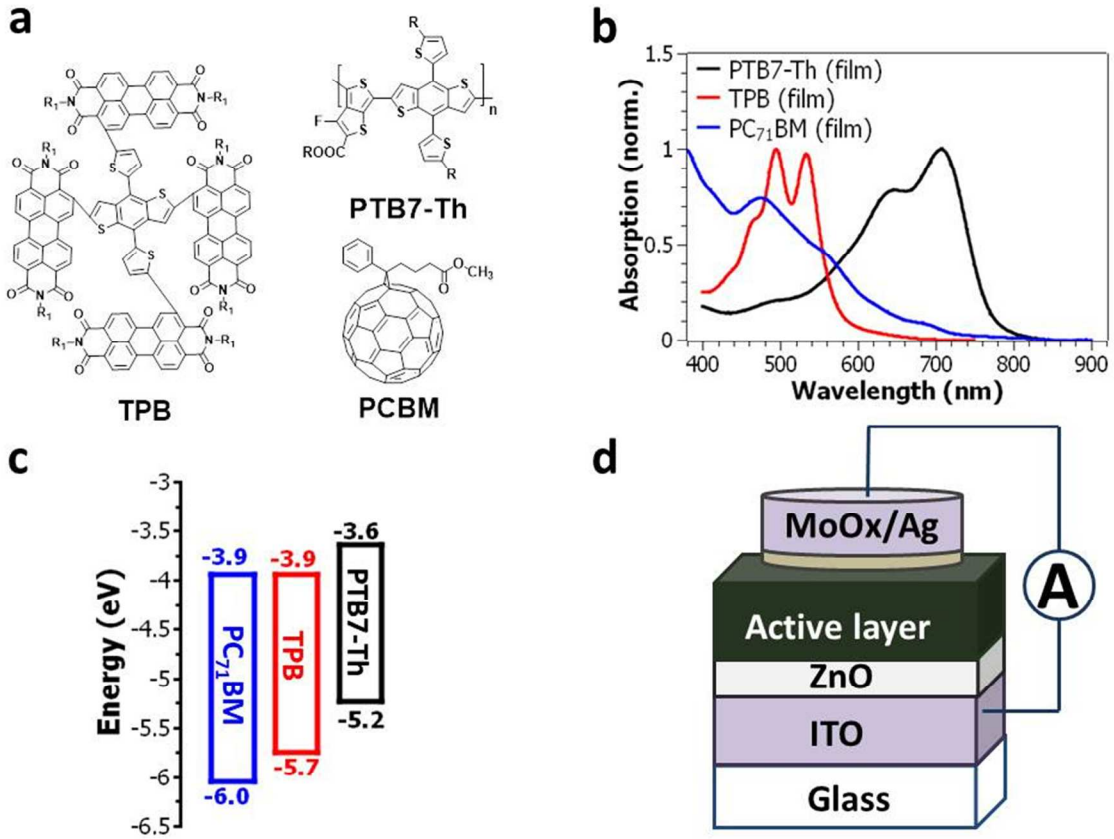

Figure 1. a) Chemical structures of TPB, PTB7-Th and $PC_{71}BM$ (R -ethylhexyl, R1 – propyl-butyl). b) Normalized absorption spectra of PTB7-Th, TPB and $PC_{71}BM$ films. c) Energy level diagram. d) Structure of solar cell device.

The molecular structure of TPB is shown in Figure 1a.[26] Figure 1b shows that the absorption spectrum of TPB is complementary to the absorption of the donor material PTB7-Th so that the blended film can harvest light from spectral range between 400 and 800 nm. In addition, we measured film fluorescence and observed a significant fluorescence quenching when even a small quantity of TPB is

added to PTB7-Th – 70% of fluorescence intensity is quenched when 10% TPB is present, which indicates electron transfer from the polymer to TPB (Figure S2). Cyclic voltammetric studies revealed a highest occupied molecular orbital (HOMO) at -5.7 eV and lowest unoccupied orbital (LUMO) at -3.9 eV (Figure 1c). Therefore, HOMO energy levels of the three components, PTB7-Th, TPB and $PC_{71}BM$, form a cascade, whereas the LUMOs of the two acceptors are very close, which allows for efficient charge transport from PTB7-Th but avoids unfavorable V_{OC} pinning in ternary devices.

To investigate the effect of the third component on OPV performances, a series of OPV devices with the varied content of TPB were fabricated. The composition was varied by increasing the concentration of the TPB (x) while keeping the weight ratio of PTB7-Th and $PC_{71}BM$ constant (PTB7-Th:TPB:$PC_{71}BM$ (1:x:1.5)). Devices had an inverted architecture consisting of ZnO/active layer/MoOx/Ag sequentially deposited onto the ITO glass substrate (Figure 1d). The experimental results of OPV performance are summarized in Table 1 and Figure 2a. The reference binary cell based on PTB7-Th:PC71BM (1:1.5) exhibited an average PCE value of 9.4%, with V_{OC} of 0.78 V, J_{SC} of 17.2 mA cm^{-2} and FF of 70%. The enhancement effect was observed even at the concentration of 5% (weight ratio related to donor) of the third component TPB. Further increase of the TPB concentration to 10% resulted in improved J_{SC} values from 17.2 to 19.4 mA/cm^{-2} while FF decreased slightly from 70% to 68%. The optimal performance with highest PCE of 10.6% was observed at this composition. Further increase of third component concentration to 30% resulted in a sharp drop of J_{SC} values from 19.4 to 13.6 mA cm^{-2}, and the corresponding OPV PCE value to 6.7%. We also tested device performance by screening different ratios of non-fullerene acceptor to $PC_{71}BM$ in a bulk heterojunction blend while keeping overall donor to acceptor ratio constant, the results are shown in Table S1.

Table 1. Summary of solar cell parameters of ternary blend devices with varying content of TPB and fixed ratio of PTB7-Th to $PC_{71}BM$ (PTB7-Th:$PC_{71}BM$:TPB 1:1.5:x). (Averaged over 12 devices).

System	V_{OC} (V)	J_{SC} (mA cm^{-2})	FF (%)	PCE^{av} (max) (%)
1:1.5:0	0.78±0.01	17.2±0.5	70±0.1	9.4±0.2 (9.8)
1:1.5:0.05	0.77±0.01	17.8±0.8	70±0.1	9.7±0.2 (10.2)
1:1.5:0.1	0.78±0.01	19.4±0.3	68±1.4	10.2±0.2 (10.6)
1:1.5:0.2	0.77±0.01	19.4±0.7	67±1.2	10.0±0.3 (10.5)
1:1.5:0.3	0.76±0.02	13.6±0.5	65±2.4	6.7±0.4 (7.5)

In order to understand the role of the third component and origin of changes in device performance, we measured external quantum efficiency (EQE) spectra of these devices. It can be seen that when TPB (10%) was added to the blend, the EQE was enhanced over a broad range of wavelength (Figure 2b). The increase in the region of 450-600 nm can be attributed to the enhanced absorption by the addition of TPB component. (Figure S1). The enhancement of EQE in PTB7-Th absorption region suggests the third component TPB facilitated extraction of charges generated in the polymer by influencing charge separation and transporting as discussed below.

The third component at the optimal concentration enhanced electron mobility. The SCLC hole mobility of devices was measured using a structure ITO/PEDOT/active layer/MoO_x/Ag and electron mobility of devices determined with a structure of ITO/ZnO/active layer/Ca/Al. The binary device exhibited the electron μ_e and hole μ_h mobilities of $(1.02 \pm 0.09) \times 10^{-5}$ $cm^2V^{-1}s^{-1}$ and $(1.03 \pm 0.13) \times$

10^{-4} $cm^2V^{-1}s^{-1}$, respectively. When the third component was added (10%), electron mobility was increased to $(3.53 \pm 0.46) \times 10^{-5}$ $cm^2V^{-1}s^{-1}$, at the same time hole mobility was $(1.01 \pm 0.09) \times 10^{-4}$ $cm^2V^{-1}s^{-1}$, showing just minor changes. The addition of non-fullerene acceptor TPB seems to facilitate mostly electron transport in the device. However, when concentration of the third component reached 30%, a significant decrease was observed in hole mobility down to $(3.31 \pm 0.43) \times 10^{-5}$ $cm^2V^{-1}s^{-1}$, resulting in lower short circuit current density, thus lower EQE and PCE.

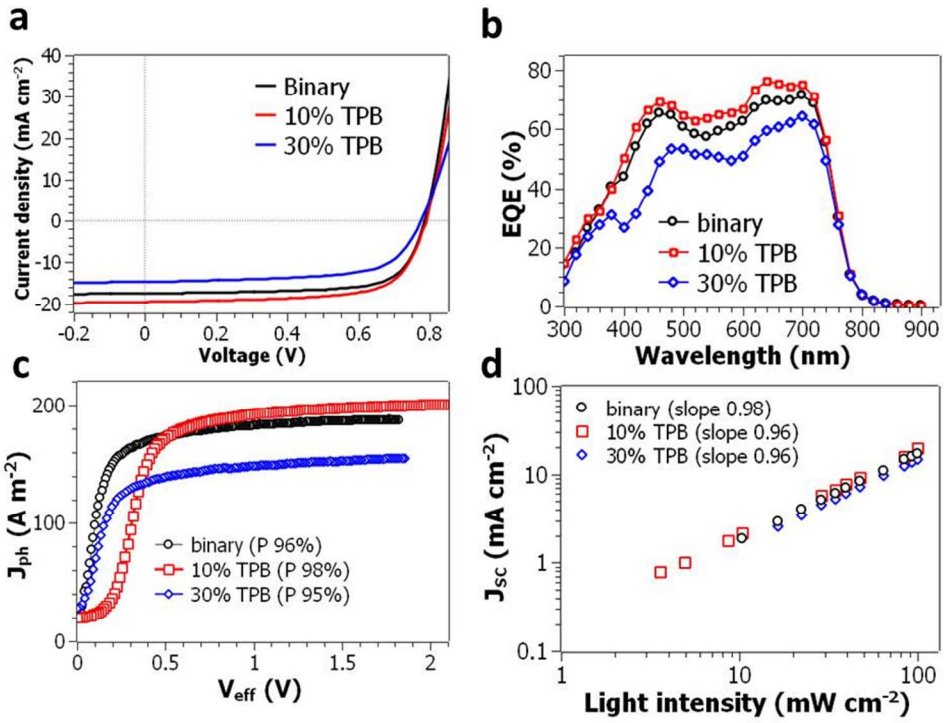

Figure 2. a) Current-voltage curves. b) External quantum efficiency spectra. c) Plot of photocurrent density versus effective voltage. d) Plot of short circuit current density versus light intensity.

Mechanistic studies

The addition of the third component only slightly affects the rate of exciton dissociation and charge generation. The exciton dissociation probability for binary and ternary devices with 10% and 30% of TPB was reflected in a plot in Figure 2c, which represents dependence of device photocurrent

density J_{ph} on an effective voltage of the device V_{eff} ($V_{eff} = V_0$-V_{appl}, where V_0 voltage where J_{ph} is zero and V_{appl} is applied voltage). It can be noted that the photocurrent increases with increasing effective voltage, reaching the saturation current, J_{sat}, at V_{eff}> 1.5 V, which depends only on the density of excitons generated in the film. It was assumed that at this point all generated excitons dissociate under applied field. The exciton dissociation probability P is determined by normalizing photocurrent density J_{ph} at short-circuit condition with a saturation current J_{sat} ($P=J_{ph\ at\ SC}/J_{sat}$). The results show that the dissociation probability showed almost no changes, 96% for binary device to 98% for device with 10% TPB, but decreased to 95% when 30% third component is added into the blend. The third component also did not show significant influence on the bimolecular recombination of the charge carriers. Under varying light intensity, the dependence of J_{SC} on incident light power will be linear if no significant bimolecular recombination is present and non-linear due to an increased charge loss through recombination. Figure 2d shows the logarithmic plot of J_{SC} vs light intensity, from which slopes >0.95 can be deduced for both binary and ternary devices. The results showed weak bimolecular recombination for these OPV systems. A slight decrease is observed from 0.98 to 0.96 when the third component is added, which is consistent with a slight FF decrease as observed in OPV properties.

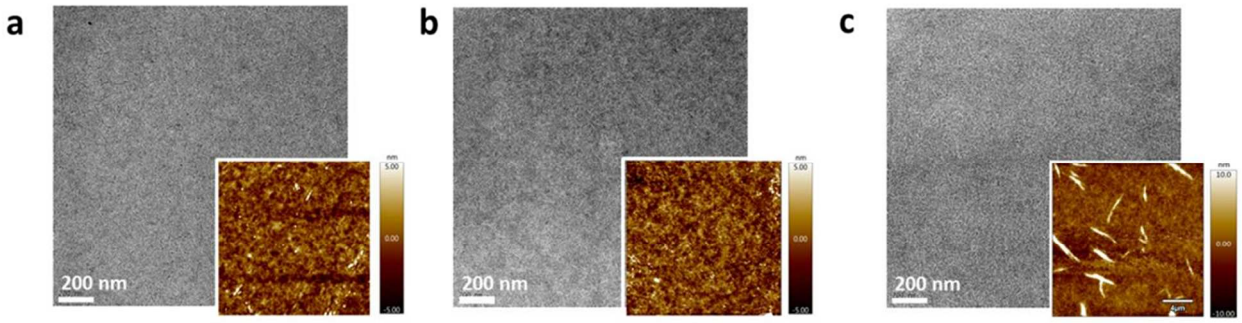

Figure 3. a) TEM and AFM ($10\mu m \times 10\mu m$) images of binary film PTB7-Th:$PC_{71}BM$. b) TEM and AFM ($10\mu m \times 10\mu m$) images of ternary film with 10% of TPB. c) TEM and AFM ($20\mu m \times 20\mu m$) images of ternary film with 30% of TPB.

Surface properties

Transmission electron microscopy (TEM) and atomic force microscopy (AFM) were employed to investigate the binary and ternary blend film morphology, and the data are summarized in Figure 3 a-c. It is observed that all blends form desired bulk heterojunction network that is beneficial for OPV performance. The addition of 10% TPB does not affect the film morphologies significantly as fibril-like structures (approximately 20 nm) are observed in both binary and 10% ternary devices. The surface roughness RMS obtained from the AFM measurements is also similar, exhibiting the values of 1.3 nm and 1.4 nm, respectively. However, upon increase of TPB content up to 30% by mass, larger aggregates are formed on the surface of the blend (Figure 3c AFM image inset) and the surface roughness RMS value increases up to 7.9 nm, indicating changes in the film morphology, which deteriorate the device performance.

We investigated surface properties further and measured surface energies of neat materials PTB7-Th, TPB and $PC_{71}BM$. We measured contact angle in a series of solvents (water, diiodomethane and ethylene glycol) on the surface of these materials in air and from there calculated surface energies. As shown in Table S3 surface energy for PTB7-Th is 34.40 mN/m, for TPB 43.43 mN/m and for $PC_{71}BM$ 46.71 mN/m. For every pair of blend's components we calculated interfacial surface energies using Neumann's equation (Table S4). For PTB7-Th/$PC_{71}BM$ interfacial surface energy was 2.325 mN/m, for PTB7-Th/TPB 1.255 mN/m and for TPB/$PC_{71}BM$ 0.168 mN/m. Surface energy and material's wetting coefficients are used as indicators which allow to determine sensitizer's location in a ternary blend.[29–31] If the wetting coefficient of a third component is larger than 1 or smaller than -1, it is preferentially located in one of the blend main component's phases. However, the wetting coefficient's value within a range from -1 to +1 indicates the preferential location of the third component being at the interface between two main components. Therefore, we calculated TPB's wetting coefficient in PTB7-Th/PCBM blend using Young's equation. For TPB wetting coefficient in PTB7-Th/$PC_{71}BM$ blend is 0.47, indicating its preferential orientation at the interfaces between PTB7-Th and $PC_{71}BM$ domains.

Film morphology studies

We also measured 2D grazing incidence wide angle x-ray scattering (GIWAXS) of films with 0, 10 and 30% TPB additive, and the data and linecuts were shown in Figure 4 (a-e). There are several main diffraction peaks observed in a GIWAXS pattern. A broad arc-like scattering near q = 0.3 $Å^{-1}$ originates from the Bragg diffraction of periodic PTB7-Th lamellar layers, whereas a peak at q_z=1.6 $Å^{-1}$ that is absent in q_y direction appears from out-of plane π-π stacking and has a preferential face-on orientation. A broad peak near q=1.4 $Å^{-1}$ originates from a $PC_{71}BM$ diffraction and appears both in out-of-plane and in-plane directions, which suggests lack of preferential orientation and rather amorphous structure. When the third component of 10% is added into a blend, an increase in intensity of these peaks was observed, which suggests an increase in crystallinity of PTB7-Th and $PC_{71}BM$ phases. This conclusion is further supported by Scherer fitting analysis of the peaks (Table S2), where correlation length for out-of-plane lamellar peak increased from 49 Å for binary blend to 52Å for ternary blend, which suggests an increased crystallinity in the blend. Similar trends were observed in in-plane direction. However, the in-plane lamellar peak intensity is significantly reduced after increasing the TPB content to 30%, while out-of-plane lamellar peak is almost unchanged. This result indicates high TPB contents are not favorable for polymer PTB7-Th taking a face-on orientation, which could harm OPV performance. The drop of $PC_{71}BM$ peak's diffraction intensity is also observed, which indicates $PC_{71}BM$ phase is disrupted. The in-plane lamellar PTB7-Th diffraction peak for binary and 10% ternary blend was observed at 0.290 $Å^{-1}$, which corresponds to d-spacing of 21.7 Å, while 30% third component shifts the peak downward a little bit, with a d-spacing of 22.1 Å. Similar trends are observed in out-of-plane direction, where lamellar distance contracts slightly when 10% TPB is present in a film (from 21.9 Å to 21.5 Å) and then expands to 22.1 Å when 30% TPB is added. The shorter polymer lamellar spacing indicates more close packing of the donor polymer, which should be beneficial for more efficient hole transport.

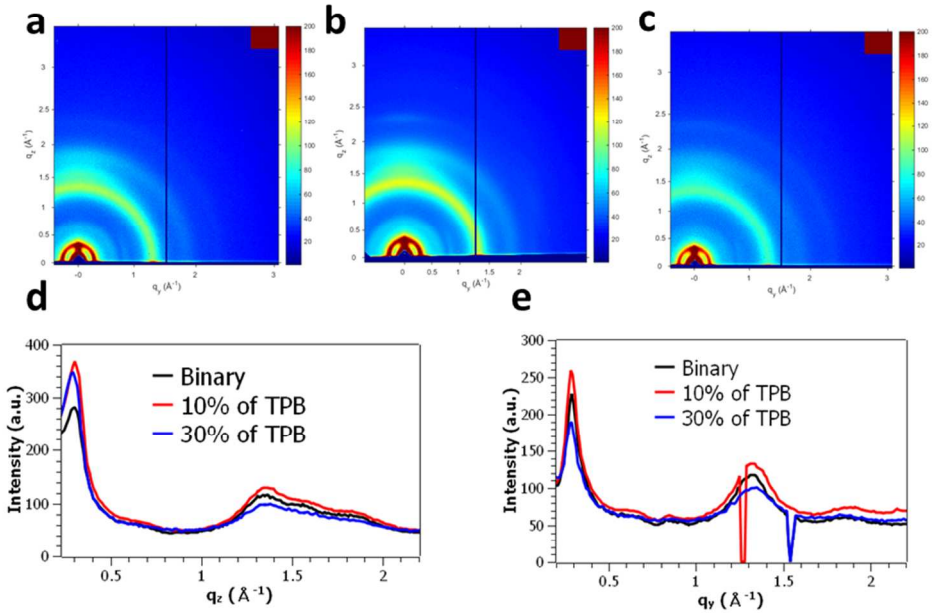

Figure 4. GIWAXS 2D patterns for a) binary blend, b) blend with 10% TPB, c) blend with 30% TPB. GIWAXS linecuts for d) out-of-plane q_z direction. e) in-plane q_y direction

Proposed model

From these studies discussed above, we propose a model (Figure 5) to explain the role that TPB plays in ternary PTB7-Th/$PC_{71}BM$ solar cells. The TPB molecule has a cross-like molecular geometry with four PDI moieties connected to BDT core. When a small amount (10%) of TPB is added to the binary PTB7-Th/$PC_{71}BM$ solar cells, TPB will preferentially stay at the interfaces between PTB7-Th and $PC_{71}BM$, as indicated by its wetting coefficient. The TPB at low concentration did not interrupt the binary system significantly, but enhanced the performances. Due to its favorable cross-like molecular geometry, TPB served as an electronic relay bridge between polymer and $PC_{71}BM$ domains, thus improving connectivity between two phases. Especially four partially conjugated PDI moieties facilitate charge separation by offering multiple charge transferring sites, which result in a much higher J_{sc} values. In addition, each TPB molecule has multiple contact points

with $PC_{71}BM$ where charge hopping can occur efficiently from TPB to $PC_{71}BM$, or from $PC_{71}BM$ to TPB because they have nearly identical LUMO energy level, leading to the higher electron mobility due to improved connectivity after 10% TPB was added.[32]

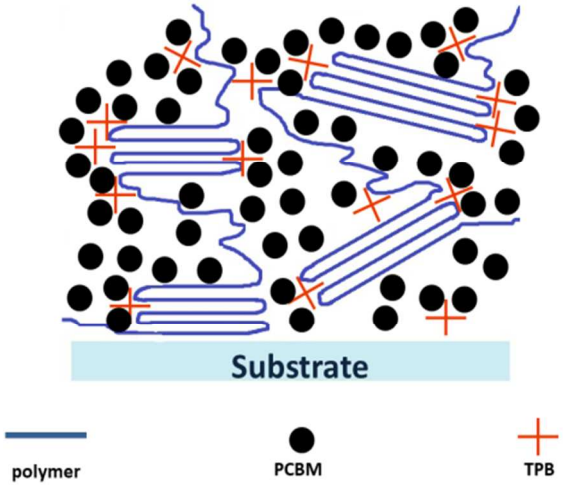

Figure 5. Schematic presentation of ternary blends where TPB serves as a linker between polymer and $PC_{71}BM$ phases.

CONCLUSION

A non-fullerene acceptor TPB was investigated as a third component in bulk heterojunction devices based on PTB7-Th and $PC_{71}BM$. It was observed that the performance of ternary devices was enhanced when 10% of TPB is added into a blend, resulting in PCE value of 10.6% for the best performing device. The observed enhancement was mostly attributed to an increase in short-circuit current of the device, originating from more efficient charge separation, increased light harvesting and increased charge mobility. A model was suggested, in which the TPB serves as an electronic relay bridge, connecting polymer and $PC_{71}BM$ phases. Four PDI units surrounding TPB's core provide multiple contact points between two phases, thus facilitating interfacial charge extraction

and improving overall device performance. The model is further supported by measurements of the interfacial surface energies that indicate TPB's preferential location at the interface between PTB7-Th and $PC_{71}BM$.

ASSOCIATED CONTENT

Supporting Information. Experimental procedures, OPV device performance data, UVVis and PL spectra, GIWAXS scattering linecut parameters, surface energy measurements, DFT calculations. This material is available free of charge via the Internet at http://pubs.acs.org.

AUTHOR INFORMATION

Corresponding Author

* E-mail: lupingyu@uchicago.edu

Present Addresses

[#] Department of Chemistry, Graduate School of Science, Osaka University, 1-1, Machikaneyama-cho, Toyonaka, Osaka 560-0043, Japan.

Author Contributions

The manuscript was written through contributions of all authors. / All authors have given approval to the final version of the manuscript. / [Δ] These authors contributed equally.

Funding Sources

This work is supported by U.S. National Science Foundation grant (NSF Grant No. DMR-1263006), DOE via the ANSER Center, an Energy Frontier Research Center funded by the U.S.

Department of Energy, Office of Science, Office of Basic Energy Sciences, under Award No. DE-SC0001059 and NIST via CHIMAD program. This work made use of the shared facilities at the University of Chicago Materials Research Science and Engineering Center, supported by National Science Foundation under award number DMR-1420709. W.C. gratefully acknowledges financial support from the U.S. Department of Energy, Office of Science, Office of Basic Energy Sciences. This research used resources of the Advanced Photon Source, a U.S. Department of Energy (DOE) Office of Science User Facility operated for the DOE Office of Science by Argonne National Laboratory under Contract No. DE-AC02-06CH11357.

Notes

The authors declare no competing financial interest.

REFERENCES

(1) Nian, L.; Gao, K.; Liu, F.; Kan, Y.; Jiang, X.; Liu, L.; Xie, Z.; Peng, X.; Russell, T. P.; Ma, Y. 11% Efficient Ternary Organic Solar Cells with High Composition Tolerance via Integrated Near-IR Sensitization and Interface Engineering. *Adv. Mater.* **2016**, *28*, 8184–8190.

(2) Zhang, G.; Zhang, K.; Yin, Q.; Jiang, X.; Zhang, G.; Zhang, K.; Yin, Q.; Jiang, X.; Wang, Z.; Xin, J.; *et al.* High-Performance Ternary Organic Solar Cell Enabled by a Thick Active Layer Containing a Liquid Crystalline Small Molecule Donor. *J. Am. Chem. Soc.* **2017**, *139*, 2387–2395.

(3) Zhao, J.; Li, Y.; Yang, G.; Jiang, K.; Lin, H.; Ade, H.; Ma, W.; Yan, H. Efficient Organic Solar Cells Processed from Hydrocarbon Solvents. *Nat. Energy* **2016**, *1*, 15027.

(4) Dai, S.; Zhao, F.; Zhang, Q.; Lau, T.-K.; Li, T.; Liu, K.; Ling, Q.; Wang, C.; Lu, X.; You,

W.; *et al.* Fused Nonacyclic Electron Acceptors for Efficient Polymer Solar Cells. *J. Am. Chem. Soc.* **2017**, *139*, 1336–1343.

(5) Baran, D.; Ashraf, R. S.; Hanifi, D. A.; Abdelsamie, M.; Gasparini, N.; Röhr, J. A.; Holliday, S.; Wadsworth, A.; Lockett, S.; Neophytou, M.; *et al.* Reducing the Efficiency-Stability-Cost Gap of Organic Photovoltaics with Highly Efficient and Stable Small Molecule Acceptor Ternary Solar Cells. *Nat. Mater.* **2017**, *16*, 363–369.

(6) Park, K. H.; An, Y.; Jung, S.; Park, H.; Yang, C. The Use of an N-Type Macromolecular Additive as a Simple yet Effective Tool for Improving and Stabilizing the Performance of Organic Solar Cells. *Energy Environ. Sci.* **2016**, *107*, 1324.

(7) Zhao, W.; Li, S.; Yao, H.; Zhang, S.; Zhang, Y.; Yang, B.; Hou, J. Molecular Optimization Enables over 13% Efficiency in Organic Solar Cells. *J. Am. Chem. Soc.* **2017**, *139*, 7148–7151.

(8) Lu, L.; Kelly, M. A.; You, W.; Yu, L. Status and Prospects for Ternary Organic Photovoltaics. *Nat. Photonics* **2015**, *9*, 491–500.

(9) An, Q.; Zhang, F.; Zhang, J.; Tang, W.; Deng, Z.; Hu, B. Versatile Ternary Organic Solar Cells: A Critical Review. *Energy Environ. Sci.* **2015**, *25*.

(10) Savoie, B. M.; Dunaisky, S.; Marks, T. J.; Ratner, M. a. The Scope and Limitations of Ternary Blend Organic Photovoltaics. *Adv. Energy Mater.* **2015**, *5*, 1400891.

(11) Ameri, T.; Khoram, P.; Min, J.; Brabec, C. J. Organic Ternary Solar Cells: A Review. *Adv. Mater.* **2013**, *25*, 4245–4266.

(12) Lu, L.; Xu, T.; Chen, W.; Landry, E. S.; Yu, L. Ternary Blend Polymer Solar Cells with Enhanced Power Conversion Efficiency. *Nat. Photonics* **2014**, *8*, 716–722.

(13) Lu, L.; Chen, W.; Xu, T.; Yu, L. High-Performance Ternary Blend Polymer Solar Cells

Involving Both Energy Transfer and Hole Relay Processes. *Nat. Commun.* **2015**, *6*, 7327.

(14) Khlyabich, P. P.; Burkhart, B.; Thompson, B. C. Efficient Ternary Blend Bulk Heterojunction Solar Cells with Tunable Open-Circuit Voltage. *J. Am. Chem. Soc.* **2011**, *133*, 14534–14537.

(15) Cheng, P.; Li, Y.; Zhan, X. Efficient Ternary Blend Polymer Solar Cells with Indene-C60 Bisadduct as an Electron-Cascade Acceptor. *Energy Environ. Sci.* **2014**, *7*, 2005.

(16) Xu, X.; Li, Z.; Wang, Z.; Li, K.; Feng, K.; Peng, Q. 10.20% Efficiency Polymer Solar Cells via Employing Bilaterally Hole-Cascade Diazaphenanthrobisthiadiazole Polymer Donors and Electron-Cascade Indene-C70 Bisadduct Acceptor. *Nano Energy* **2016**, *25*, 170–183.

(17) Zhang, J.; Zhao, Y.; Fang, J.; Yuan, L.; Xia, B.; Wang, G.; Wang, Z.; Zhang, Y.; Ma, W.; Yan, W.; *et al.* Enhancing Performance of Large-Area Organic Solar Cells with Thick Film via Ternary Strategy. *Small* **2017**, *13*, 1–8.

(18) An, Q.; Zhang, F.; Sun, Q.; Zhang, M.; Zhang, J.; Tang, W.; Yin, X.; Deng, Z. Efficient Organic Ternary Solar Cells with the Third Component as Energy Acceptor. *Nano Energy* **2016**, *26*, 180–191.

(19) Lu, H.; Zhang, J.; Chen, J.; Liu, Q.; Gong, X.; Feng, S.; Xu, X.; Ma, W.; Bo, Z. Ternary-Blend Polymer Solar Cells Combining Fullerene and Nonfullerene Acceptors to Synergistically Boost the Photovoltaic Performance. *Adv. Mater.* **2016**, *28*, 9559–9566.

(20) Liu, T.; Guo, Y.; Yi, Y.; Huo, L.; Xue, X.; Sun, X.; Fu, H.; Xiong, W.; Meng, D.; Wang, Z.; *et al.* Ternary Organic Solar Cells Based on Two Compatible Nonfullerene Acceptors with Power Conversion Efficiency >10%. *Adv. Mater.* **2016**, *28*, 10008–10015.

(21) Zhang, Y.; Deng, D.; Lu, K.; Zhang, J.; Xia, B.; Zhao, Y.; Fang, J.; Wei, Z. Synergistic

Effect of Polymer and Small Molecules for High-Performance Ternary Organic Solar Cells. *Adv. Mater.* **2015**, *27*, 1071–1076.

(22) Goh, T.; Huang, J. S.; Yager, K. G.; Sfeir, M. Y.; Nam, C. Y.; Tong, X.; Guard, L. M.; Melvin, P. R.; Antonio, F.; Bartolome, B. G.; *et al.* Quaternary Organic Solar Cells Enhanced by Cocrystalline Squaraines with Power Conversion Efficiencies >10%. *Adv. Energy Mater.* **2016**, *6*, 1600660.

(23) Cnops, K.; Rand, B. P.; Cheyns, D.; Verreet, B.; Empl, M. A.; Heremans, P. 8.4% Efficient Fullerene-Free Organic Solar Cells Exploiting Long-Range Exciton Energy Transfer. *Nat. Commun.* **2014**, *5*, 3406.

(24) Zhao, F.; Luo, X.; Liu, J.; Du, L.; Lv, W.; Sun, L.; Li, Y.; Wang, Y.; Peng, Y. Toward High Performance Broad Spectral Hybrid Organic–inorganic Photodetectors Based on Multiple Component Organic Bulk Heterojunctions. *J. Mater. Chem. C* **2016**, *4*, 815–822.

(25) Liu, T.; Xue, X.; Huo, L.; Sun, X.; An, Q.; Zhang, F.; Russell, T. P.; Liu, F.; Sun, Y. Highly Efficient Parallel-Like Ternary Organic Solar Cells. *Chem. Mater.* **2017**, *29*, 2914–2920.

(26) Wu, Q.; Zhao, D.; Schneider, A. M.; Chen, W.; Yu, L. Covalently Bound Clusters of Alpha-Substituted PDI-Rival Electron Acceptors to Fullerene for Organic Solar Cells. *J. Am. Chem. Soc.* **2016**, *138*, 7248–7251.

(27) Wu, Q.; Zhao, D.; Goldey, M. B.; Filatov, A. S.; Sharapov, V.; Colon, Y. J.; Cai, Z.; Chen, W.; de Pablo, J. J.; Galli, G.; Yu, L. Intra-Molecular Charge Transfer and Electron Delocalization in Non-Fullerene Organic Solar Cells. *ACS Appl. Mater. Interfaces* **2018**, *10*, 10043–10052.

(28) Lee, B. R.; Jung, E. D.; Nam, Y. S.; Jung, M.; Park, J. S.; Lee, S.; Choi, H.; Ko, S.-J.;

Shin, N. R.; Kim, Y.-K.; *et al.* Amine-Based Polar Solvent Treatment for Highly Efficient Inverted Polymer Solar Cells. *Adv. Mater.* **2014**, *26*, 494–500.

(29) Honda, S.; Ohkita, H.; Benten, H.; Ito, S. Selective Dye Loading at the Heterojunction in Polymer/Fullerene Solar Cells. *Adv. Energy Mater.* **2011**, *1*, 588–598.

(30) Ameri, T.; Khoram, P.; Heumüller, T.; Baran, D.; Machui, F.; Troeger, A.; Sgobba, V.; Guldi, D. M.; Halik, M.; Rathgeber, S.; *et al.* Morphology Analysis of near IR Sensitized Polymer/fullerene Organic Solar Cells by Implementing Low Bandgap Heteroanalogue C-/Si-PCPDTBT. *J. Mater. Chem. A* **2014**, *2*, 19461–19472.

(31) Zhu, Y.; Chen, Y.; Zhao, S.; Huang, Y.; Xu, Z.; Qiao, B.; Zhao, J.; Li, Y.; Liu, J.; Xu, X. The Effects of SQ Additive on Charge Carrier Transport and Recombination in PCDTBT:PC71BM Based Ternary Organic Solar Cells. *Synth. Met.* **2017**, *234*, 125–131.

(32) Foster, S.; Deledalle, F.; Mitani, A.; Kimura, T.; Kim, K. B.; Okachi, T.; Kirchartz, T.; Oguma, J.; Miyake, K.; Durrant, J. R.; *et al.* Electron Collection as a Limit to polymer:PCBM Solar Cell Efficiency: Effect of Blend Microstructure on Carrier Mobility and Device Performance in PTB7:PCBM. *Adv. Energy Mater.* **2014**, *4*, 1400311.